Published in final edited form as:
J Am Chem Soc. 2013 February 6; 135(5): 1816–1822. doi:10.1021/ja309557s.

Inhibition of IspH, a $[4Fe\text{-}4S]^{2+}$ enzyme involved in the biosynthesis of isoprenoids via the MEP pathway

Karnjapan Janthawornpong[†,‡], **Sergiy Krasutsky**[§,‖,‡], **Philippe Chaignon**[†], **Michel Rohmer**[†], **C. Dale Poulter**[§,*], and **Myriam Seemann**[†,*]

[†]Université de Strasbourg, CNRS UMR 7177, Institut Le Bel, 4 rue Blaise Pascal, CS 90032, 67081 Strasbourg Cedex, France

[§]Department of Chemistry, University of Utah, 315 South 1400 East RM 2020, Salt Lake City, Utah 84112, United States

Abstract

The MEP pathway, which is absent in animals but present in most pathogenic bacteria, in the parasite responsible for malaria and in plant plastids, is a target for the development of antimicrobial drugs. IspH, an oxygen-sensitive [4Fe-4S] enzyme, catalyzes the last step of this pathway and converts (*E*)-4-hydroxy-2-methylbut-2-enyl 1-diphosphate (HMBPP) into the two isoprenoid precursors: isopentenyl diphosphate (IPP) and dimethylallyl diphosphate (DMAPP). A crucial step in the mechanism of this enzyme is the binding of the C4 hydroxyl of HMBPP to the unique fourth iron site in the $[4Fe\text{-}4S]^{2+}$ moiety. Here we report the synthesis and the kinetic investigations of two new extremely potent inhibitors of *E. coli* IspH where the OH group of HMBPP is replaced by an amino and a thiol group. (*E*)-4-Mercapto-3-methyl-but-2-en-1-yl diphosphate is a reversible tight-binding inhibitor of IspH with $K_i = 20 \pm 2$ nM. A detailed kinetic analysis revealed that (*E*)-4-amino-3-methylbut-2-en-1-yl diphosphate is a reversible slow-binding inhibitor of IspH with $K_i = 54 \pm 19$ nM. The slow binding behavior of this inhibitor is best described by a one-step mechanism with the slow step consisting in the formation of the enzyme-inhibitor (EI) complex.

INTRODUCTION

Isoprenoid compounds constitute the most chemically diverse family of natural products and are found in all living organisms. The carbon skeletons of isoprenoid molecules are derived from polyisoprenoid chains formed by the repeated additions of isopentenyl diphosphate (**IPP, 1**) to dimethylallyl diphosphate (**DMAPP, 2**). These two building blocks are synthesized by two different routes: the well-established mevalonate pathway[1] known since the late fifties and the more recently discovered methylerythritol phosphate (**MEP**) pathway.[2,3] In this latter pathway, **IPP** and **DMAPP** are carbohydrate derivatives synthesized from pyruvate (**3**) and D-glyceraldehyde phosphate (**4**) *via* 1-deoxy-D-xylulose 5-phosphate (**5**), 2-*C*-methyl-D-erythritol 4-phosphate (**6**), 4-diphosphocytidyl-2-*C*-methyl-

Corresponding Author: mseemann@unistra.fr; poulter@chemistry.utah.edu.
‖**Present Addresses:** sergiy.krasutsky@amriglobal.com, AMRI Global, Inc. 26 Corporate Circle, P.O. Box, 15098, Albany, NY, 12212-5098
‡These authors contributed equally.

Author Contributions
The manuscript was written through contributions of all authors. / All authors have given approval to the final version of the manuscript. /

Supporting Information. Figures S1–S6. Table S1, synthetic procedures, and NMR spectra for synthetic intermediates. This material is available free of charge via the Internet at http://pubs.acs.org.

D-erythritol (**7**), 4-diphosphocytidyl-2-*C*-methyl-D-erythritol 2-phosphate (**8**), 2-*C*-methyl-D-erythritol 2,4-cyclodiphosphate (**9**) and (*E*)-4-hydroxy-2-methylbut-2-en-1-yl diphosphate (**HMBPP**, **10**) (Scheme 1).

The MEP pathway is found in most bacteria, including *Mycobacterium tuberculosis* responsible for tuberculosis, in the malaria parasite *Plasmodium falciparum*, and in the chloroplasts of plants. The MEP pathway is absent in humans and therefore presents an appealing target for the development of new antimicrobials and for herbicides because it provides essential elements for the photosynthetic apparatus.[4,5] Fosmidomycin inhibits the second enzyme of the pathway, deoxyxylulose phosphate reductoisomerase (DXR), and is effective alone[6] or in combination with clindamycin[7] or artesunate[8] for the treatment of uncomplicated malaria in humans. To date, fosmidomycin is the only inhibitor of the MEP pathway that is being investigated clinically. Our interest in the MEP pathway as a target for new therapeutic agents, led us to the design of new chemical tools to study the reactions catalyzed by IspH, the last enzyme of the MEP pathway.

IspH contains an oxygen-sensitive $[4Fe\text{-}4S]^{2+}$ iron-sulfur center and catalyses the conversion of **HMBPP** (**10**) to a mixture of **IPP** (**1**) and **DMAPP** (**2**) (for reviews see ref 9 and 10).

The $[4Fe\text{-}4S]^{2+}$ cluster in *E. coli* IspH was identified by EPR spectroscopy after reconstitution of the enzyme with $FeCl_3$, Na_2S and DTT in an oxygen-free atmosphere. [11] This result was confirmed by field-dependent Mössbauer spectroscopy, indicating that IspH contains an unusual $[4Fe\text{-}4S]^{2+}$ cluster *in vivo* with one iron atom linked to three inorganic sulfur atoms from the cluster and to two or three non-sulfur ligands (O and/or N).[12] The first X-ray structures reported for IspH from *Aquifex aeolicus*[13] and E*scherichia. coli*[14] contained a [3Fe-4S] cluster and, hence, were incomplete. A structure of *E. coli* IspH with an intact [4Fe-4S] cluster was only obtained as a complex with the substrate **HMBPP**.[15]

The mechanism catalyzed by IspH requires i) removal of a hydroxyl group, ii) transfer of two electrons from the [4Fe-4S] cluster, and iii) the protonation of an intermediate allylic anion[16]. Mössbauer spectroscopy[12] and an X-ray structure of the *E. coli* IspH:**HMBPP** complex[15] provided the first evidence for binding of the OH group in **HMBPP** to the unique fourth iron site of the $[4Fe\text{-}4S]^{2+}$ cluster of IspH. EPR and ENDOR spectroscopy performed on a reduced inactive IspH mutant[17] and X-ray irradiation of IspH:**HMBPP** complex crystal[15] supports the formation of organometallic intermediates.

We synthesized two **HMBPP** analogues where the OH group was replaced by an amino or a thiol group known to coordinate iron atoms in order to further study the reaction catalyzed by IspH (Scheme 2). These moieties are known to coordinate to iron atoms and are poor leaving groups relative to hydroxyl. The binding mechanisms by which these molecules inhibit *E. coli* IspH were investigated by kinetic studies.

RESULTS AND DISCUSSION

Synthesis of TMBPP and AMBPP

The divergent synthesis of **TMBPP** and **AMBPP** from THP-protected *E*-2-methyl-2-butene-1,4-diol (**16**) is outlined in Scheme 3. Diethyl L-tartrate (**13**) was cleaved with periodate and the resulting aldehyde was trapped in situ with the 2-(triphenylphosphoranylidene) ylid of propanal,[18,19] followed by reduction with $NaBH_4$ to give hydroxy ester **14**. After protection of the alcohol as a t-butyldimethylsilyl ether, the ester moiety was reduced with DIBAL. The resulting alcohol was protected as a THP ether, and the t-butyldimethylsilyl group removed by treatment with fluoride to give **16. TMBPP**

was synthesized from **16** by converting the hydroxyl group to the corresponding chloride, followed by treatment with potassium thioacetate. In order to circumvent problems with oxidation of the thiol moiety during the remaining steps, the thioacetate was converted to the mixed 2-pyridyl disulfide and the THP group was removed to give **18**. We initially attempted to introduce the diphosphate moiety by the procedure of Davisson *et al.*[20] but were unable to prepare the intermediate chloride from **18** and instead resorted to the less efficient Cramer phosphorylation.[21] Mixed disulfide **19** was stored at −80°C and **TMBPP** was prepared immediately before use by treatment with DTT.

AMBPP was prepared by displacement of the hydroxyl group in **16** with phthalimide, followed by treatment with hydrazine to give amine **20**. The amine was converted to the corresponding Fmoc carbamate and the THP group removed to give alcohol **21**. The alcohol was converted to the corresponding diphosphate as described for **TMBPP**, and the Fmoc group removed with piperidine to give **AMBPP**.

IspH

IspH was produced from *E. coli* strain M15[pREP4, pQE30-IspH] as a His_6-tagged protein and was purified to homogeneity on a Ni^{2+}-resin affinity column in a glove box with a nitrogen atmosphere containing less than 2 ppm oxygen. The UV/visible spectrum of the protein, the iron and sulfur content, and Mössbauer spectra were identical to those previously reported[12] and confirmed that the protein contained an intact $[4Fe\text{-}4S]^{2+}$ cluster. IspH catalyzed the reduction of **HMBPP** to a mixture of **IPP** and **DMAPP** (Scheme 1). This reaction was coupled to a system that reduced the oxidized $[4Fe\text{-}4S]^{2+}$ cluster. In *E. coli* reduction is facilitated by the natural flavodoxin/ flavodoxin reductase/NADPH system.[11,22] In vitro, reduction can also be performed chemically with the semiquinone radical of 5-deazaflavin,[11,22] dithionite (DT) reduced methylviologen (MV), or other dithionite reduced redox mediators.[23] Using a spectroscopic assay based on the change in NADPH absorbance at 340 nm and optimal concentrations of NADPH, flavodoxin reductase (FpR1) and flavodoxine (FldA) in 50 mM Tris HCl buffer, pH 8, IspH activity was approximately 800 $nmol.min^{-1}.mg^{-1}$, in accordance with previously reported values.[12, 24]

TMBPP and AMBPP are not substrates for IspH

IspH was assayed for turnover under anaerobic conditions by monitoring the absorbance at 340 nm for incubations containing 200 μM **HMBPP**, **TMBPP** or **AMBPP** (as a control). Figure 1 shows that IspH was fully active in the presence of **HMBPP**. Although the rate of NADPH consumption was twice the rate of NADPH degradation in the presence of **TMBPP** or **AMBPP** in a control assay containing no substrate with identical concentrations of cofactors and enzyme during the first two minutes, no differences were seen afterwards, suggesting that the thiol and amino analogues are not substrates for IspH.

Inhibition of IspH by TMBPP and AMBPP

Preliminary experiments were conducted to determine IC_{50} values for **TMBPP** and **AMBPP** using two different IspH assays performed under anaerobic conditions. In the first assay, activity was monitored using [3-^{14}C]**HMBPP** and the biological reducing system NADPH/FpR1/FldA. The products were quantified by liquid scintillation spectrometry upon dephosphorylation of **IPP** and **DMAPP** with alkaline phosphatase, releasing isopentenol and dimethylallyl alcohol, followed by selective heptane extraction of the monoalcohols.[11] In the second assay, IspH activity was determined using dithionite-reduced methylviologen (DT-reduced MV) as the reducing agent and by monitoring the decrease of the absorbance of reduced methylviologen at 732 nm.[17,25] As shown in Table 1, **TMBPP** and **AMBPP** are good inhibitors of IspH with IC_{50} values below 0.5 μM. A series of alkynes[26] and pyridine

diphosphates [27] were previously tested as IspH inhibitors using DT-reduced MV as reducing system and the same experimental conditions as described in Table 1 (conditions b). According to these studies, 3-butynyl diphosphate was the best inhibitor of IspH with IC_{50} = 450 nM for the *Aquifex aeolicus* enzyme. The respective IC_{50} values of 210 nM and 150 nM for **TMBPP** and **AMBPP** (Table 1, conditions b) with *E. coli* IspH indicate that the compounds are potent inhibitors.

Steady-state inhibition studies of IspH with **TMBPP** were performed using the biological reducing system NADPH/FpR1/FldA and [3-^{14}C]**HMBPP**. The results show that **TMBPP** is a competitive inhibitor of IspH with K_i = 20 ± 2 nM (Figure S1). Using a centrifugal filter (Microcon Y-10), **TMBPP** was removed from the inhibited IspH·**TMBPP** complex by several centrifugation-dilution cycles during which the enzyme regained its activity, confirming that **TMBPP** is a reversible tight-binding inhibitor.

Preliminary experiments were performed to check the ability of **AMBPP** to inhibit IspH using NADPH/FpR1/FldA as a reducing system by monitoring the decrease of absorbance at 340 nm. The progress curves obtained when the reaction was initiated by addition of **HMBPP** or by IspH were different (Figure 2). Upon initiation by addition of IspH, the progress curve displayed a marked curvature during the first 3–5 min, followed by linear rate of turnover. However, when the enzyme was first incubated with **AMBPP** before addition of **HMBPP**, the progress curve was linear. The linear regions of both progress curves (a and b in Figure 2) had the same slope. This behavior is typical for a reversible slow-binding inhibitor.[28,29] The reversibility of the inhibition was confirmed by removing the inhibitor from the IspH·**AMBPP** complex as described above for **TMBPP**.

Rates were measured by the decrease in NADPH absorbance at 340 nm for varied **AMBPP** concentrations at a fixed concentration of **HMBPP**. Due to limitations of working in an anaerobic environment, approximately 30 s were needed to add enzyme and mix the sample. Accordingly, 30 s were added to the time of each run. Progress curves, for formation of the products in the presence of different **AMBPP** concentrations (Figure 3), were generated and fitted to Eqn (1) (see materials and methods).

Several mechanisms have been proposed for reversible competitive slow binding inhibition.[28–30] The two widely accepted models involve slow addition of the inhibitor (I) to the enzyme to form an E·I complex (mechanism A, see experimental procedures) or rapid formation of E·I followed by a slow conformational change to form an E·I* complex (mechanism B, see experimental procedures). The two mechanisms can be distinguished from relationships among the initial rate (v_0), the steady-state rate (v_s) and the apparent first-order rate constant for inhibition (k_{app}) as a function of inhibitor concentration.[28–30] In mechanism A, formation of E·I is slow. The initial v_0 rate is independent of [I], and $1/v_s$ and k_{app} are linear functions of [I]. In mechanism B, the formation of the E·I complex is fast and undergoes a slow isomerization to E·I *. $1/v_0$ and $1/v_s$ are linear functions of [I] and k_{app} is a hyperbolic function of [I] with limiting values of k_6 and k_5+k_6.

A plot of the apparent first-order rate constant (k_{app}) versus inhibitor concentration was linear (Figure 3B). The reciprocal plot of the steady-state rate ($1/v_s$) versus [**AMBPP**] was linear and v_0 was independent of [I] (Figure 1S and 2S). Fitting the experimental data to the equation for mechanism A (Eqn (2)) with K_m^{HMBPP} = 1 μM gave $k_3 = 4.1 \times 10^4\ M^{-1}s^{-1}$, $k_4 = 2.2 \times 10^{-3}\ s^{-1}$, and K_i = 54 ± 19 nM. Thus, inhibition of IspH appears to proceed by slow addition of **AMBPP** to free IspH and not a conformational change of the enzyme-inhibitor complex. The competitive inhibition was confirmed using the radioactive assay and varying concentrations of [3-^{14}C]**HMBPP** and **AMBPP**. IspH and **AMBPP** were preincubated before the assays were initiated by the addition of the substrate. Double-reciprocal plots of

velocity versus substrate concentration at different concentrations of **AMBPP** are given in Figure S4. The competitive inhibition constant was estimated to be 35 nM ± 8 nM

Similar values for K_i were obtained by analysis of data from the progress curves and the Lineweaver-Burk plot. The relatively small difference in K_i probably results from experimental difficulties related to having to handle an unstable enzyme in a glove box. The inhibition constant for **AMBPP** and the rate of binding to IspH both appear to decrease as pH increases (Figures S5 and S6), suggesting that **AMBPP** is a better inhibitor in the non-protonated amine form. Due to the instability of IspH, K_i for **AMBPP** could not be determined at higher pHs.

Mechanistic Considerations

The slow binding behavior of **AMBPP** may reflect a requirement that the free amine binds to the enzyme. Mössbauer studies of IspH in the presence of either **TMBPP** and **AMBPP** indicate that the inhibitors coordinate to the unique non-sulfur tetracoordinated iron in the $[4Fe\text{-}4S]^{2+}$ cluster of the enzyme through their respective thiol and amino groups.[31] Thus, the slow binding behavior seen for **AMBPP** at pH 8, but not for **TMBPP**, is consistent with binding of the free amine and thiol, respectively, to the $[4Fe\text{-}4S]^{2+}$ cluster.

The X-ray structure of the IspH·**HMBPP** complex[15], data from Mössbauer spectroscopy,[12,31] and evidence obtained in this work, indicate that **HMBPP** binds to the $[4Fe\text{-}4S]^{2+}$ cluster in IspH. Analysis of incorporation of deuteriated isotopologues of 1-deoxy-D-xylulose into pentelene during feeding experiments with *Streptomyces avermitilis*[32] as well as crystallographic studieas of several IspH mutants in complex with the substrate[33] indicates that the CH_2OH group in **HMBPP** undergoes a rotation by almost 180° to position the hydroxyl group to interact with E124. An EPR/ENDOR study of the dithionite reduced inactive E124A mutant of *A. aeolicus* IspH in the presence of **HMBPP** suggests that a one electron transfer to the $[4Fe\text{-}4S]^{2+}$ cluster in the IspH·**HMBPP** complex results in a rearrangement to give a η^2-alkenyl complex (Scheme 4).[17] Nevertheless, the structure of the η^2-alkenyl complex, assigned according to ^{13}C-ENDOR studies of the E126A IspH mutant incubated with [U-^{13}C]HMBPP, is being challenged by Duin *et al.* with respect to the observed ^{13}C couplings (1.7 and 0.8 MHz) that might be larger.[34] Proton transfer to the hydroxyl group and elimination of water and electron transfer, either simultaneously or sequentially, could generate the η^3-allyl (π) complex [10,15,17,22] (Scheme 4). During X-ray exposure of the IspH:**HMBPP** complex, an intermediate lacking the OH group and coordinated to the apical iron of the [4Fe-4S] *via* its double bound was observed although the mode of bonding between the hydrocarbon moiety and iron could not be determined from the crystallographic data.[10,15] EPR, ^{31}P and ^{2}H ENDOR investigations of one-electron reduced *A. aeolicus* IspH in presence of HMBPP provided evidence for the formation of a new reaction intermediate with spectroscopic properties similar to the $[4Fe\text{-}4S]^{3+}$ found in ferredoxin:thioredoxin reductase.[34] This latter intermediate was recently proposed to be the η^3-allyl (π) complex linked to a $[4Fe\text{-}4S]^{3+}$.[35] Subsequently, protonation of the η^3-allyl (π) complex at the *si* face of C-2 will give IPP while protonation at C-4 will give DMAPP (Scheme 4).[11,16]

Elimination of water from **HMBPP** is a crucial step in the formation of the putative η^3-allyl (π) complex. While the reactivity of the metallocyclopropyl η^2-alkenyl intermediate toward elimination should be enhanced by one-electron reduction, it is not known if transfer of the second electron and elimination events are synchronous or stepwise. The inhibitors of IspH characterized in this work were designed to replace the hydroxyl moiety in **HMBPP** with less reactive amine and thiol leaving groups. As such, they are good tools to further investigate the IspH mechanism and we anticipate that Mössbauer, EPR, X-ray studies of

reduced IspH in complex with **TMBPP** and **AMBPP** might provide further information about the putative η^2-alkenyl complex, especially **AMBPP**, by blocking the elimination step with concomitant accumulation of the η^2-alkenyl complex.

CONCLUSIONS

In summary, we report the synthesis of (*E*)-4-thio-3-methylbut-2-enyl 1-diphosphate (**TMBPP, 11**) and (*E*)-4-amino-3-methylbut-2-enyl 1-diphosphate (**AMBPP, 12**)[36], two **HMBPP** analogues, where the OH group is replaced by poorer thiol and amino leaving groups, respectively. Both compounds are potent inhibitors of *E. coli* IspH, an enzyme containing an oxygen sensitive [4Fe-4S] cluster that catalyzes the final step in the **MEP** route to **IPP** and **DMAPP**. A steady-state kinetic study of inhibition of IspH by **TMBPP** shows that the molecule is a potent competitive reversible inhibitor with K_i = 24 nM. **AMBPP** is also a reversible competitive inhibitor; however, the molecule shows slow binding behavior where the slow step is formation of an IspH·**AMBPP** complex (K_i = 54 nM). We suggest that the origin of the slow binding behavior is related to the fact that the free amino group in **AMBPP** binds to the fourth iron site of the $[4Fe\text{-}4S]^{2+}$ cluster of IspH and deprotonation of the dominant protonated form of **AMBPP** at physiological pH is a required step. Accordingly, **TMBPP** (IC_{50} = 210 nM) and **AMBPP** (IC_{50} = 150 nM) are substantially more potent IspH inhibitors than the previously reported alkynyl diphosphates (IC_{50}= 0.45 μM for 3-butynyl diphosphate with *Aquifex aeolicus* IspH)[26] and pyridine phosphates (IC_{50} = 38 μM for BPH-293 with *Aquifex aeolicus* IspH)[27], which also bind to the [4Fe-4S] cluster.

EXPERIMENTAL PROCEDURES

(*E*)-4-Mercapto-3-methyl-but-2-en-1-yl diphosphate bis ammonium salt (TMBPP, 11)

To (*E*)-3-methyl-4-(pyridin-2-yldisulfanyl)-but-2-en-1-yl 1-diphosphate **19** (50 mg, 0.12 mmol) in 100 mM NH_4HCO_3 (1 mL) was added dithiothreitol (DTT, 55 mg, 0.36 mmol) in 100 mM NH_4HCO_3 (1 mL). After stirring for 1 h at rt, the mixture was lyophilized, and the residue was chromatographed on cellulose with elution by 100 mM NH_4HCO_3:iPrOH (2:8 v/v). The fractions were analyzed by silica TLC (iPrOH:H_2O:NH_4OH (6:1:3 v/v/v)) and visualized by *p*-anisaldehyde. The fractions containing the product were combined, concentrated under reduced pressure, and then lyophilized to give a white solid (17 mg, 90%); R_f 0.32 (iPrOH:H_2O:NH_4OH (6:1:3 v/v/v)); ^{1}H NMR (D_2O) 1.79 (3H, s), 3.18 (2H, s), 4.47 (2H, t, J = 8 Hz), 5.62 (1H, m); ^{13}C NMR (D_2O) 14.45, 32.37, 62.64 (d, $J_{C,P}$ = 5 Hz), 121.94 (d, $J_{C,P}$ = 8 Hz), 125.12; ^{31}P NMR (D_2O) − 9.73 (d, J = 22 Hz), −6.92 (d, J = 22 Hz); HRMS (MALDI) calcd. for $C_5H_{11}O_7SP_2$ [M-H] 276.97062, found 276.97112.

(*E*)-4-Amino-3-methylbut-2-enyl 1-diphosphate bis ammonium salt (AMBPP, 12)

To (*E*)-(2-methyl-but-2-enyl)-carbamic acid 9H-fluoren-9-yl methyl ester 4-diphosphate **27** (120 mg, 0.23 μmol) was added piperidine (5 mL). After stirring for 1 h at rt, piperidine was removed at reduced pressure and the residue was purified by flash chromatography on 230–400 mesh silica with elution by iPrOH:H_2O:NH_4OH (6:0.5:2.5 v/v/v). The fractions were analyzed by silica TLC (iPrOH:H_2O:NH_4OH (6:1:3 v/v/v)) and visualized by *p*-anisaldehyde. The fractions containing the product were combined, concentrated under reduced pressure, and then lyophilized to give a white solid (58 mg, 85%); R_f 0.1 (iPrOH:H_2O:NH_4OH (6:1:3 v/v/v)); ^{1}H NMR (D_2O) 1.53 (3H, s), 3.07 (2H, s), 4.32 (2H, t, J = 8 Hz), 5.41 (1H, m); ^{13}C NMR (D_2O) 14.36, 45.51, 62.17 (d, $J_{C,P}$ = 5 Hz), 125.58 (d, $J_{C,P}$ = 8 Hz), 131.94; ^{31}P NMR (D_2O) − 9.73 (d, J = 22 Hz), −6.92 (d, J = 22 Hz); HRMS (MALDI) calcd. for $C_5H_{12}NO_7P_2$ [M-H] 260.0095, found 260.0092.

Purification of IspH

The *ispH* gene of *E. coli* was cloned into pQE-30 (Qiagen) as previously described.[11] The resulting pQE30-IspH plasmid was used to transform *E. coli* M15 [pREP4] to give *E. coli* M15 strain [pREP4, pQE30-IspH]. *E. coli* M15 [pREP4, pQE30-IspH] was grown at 30°C on LB medium (6×500 mL) containing ampicillin (100 μg mL^{-1}) and kanamycin (25 μg mL^{-1}) to 0.6 OD_{600}. $FeCl_3$ (100 μM) was then added and protein synthesis was induced with IPTG (100 μM) for 4 h at 30°C. Cells were harvested by centrifugation (7000 g, 10 min) and kept at −80°C until used.

The following steps were carried out in a glove box (Jacomex BS531 T2) equipped with an oxymeter (ARELCO ARC) and filled with a nitrogen atmosphere containing less than 2 ppm O_2. *E. coli* M15 [pREP4, pQE30-IspH] cells (11 g) were suspended in 50 mM Tris-HCl buffer (20 mL, pH 8), and sonicated (6×40 s with 1 min cooling). After centrifugation (15000 g, 15 min), the supernatant was collected and loaded onto an Ni^{2+}-NTA column (Qiagen, 1.2 cm x 7 cm column), equilibrated with 50 mM Tris-HCl bufer, pH 8. The resin was first washed with 50 mM Tris-HCl buffer, pH 8, containing 20 mM imidazole solution followed by same buffer containing 30 mM imidazole (20 mL). The His_6-IspH protein was eluted with Tris buffer (8 mL, pH 8) containing 100 mM imidazole to give IspH (27 mg) after pooling the most colored and pure fractions (purity >90% as judged by SDS-polyacrylamide gel electrophoresis). After concentration on Microcon YM-30 (Millipore), the resulting brown-green protein solution (3 mL, 9 mg. mL^{-1}) was divided in aliquots and stored in liquid nitrogen. Protein concentration was measured by the method of Bradford using bovine serum albumin as a standard.[38] Iron was quantified by the method of Fish[39] and sulphide as described by Beinert. [40]

Spectrophotometric IspH assay using NADPH/FpR1/FldA as reducing system

HMBPP was synthesized as previously decribed.[41] In a typical IspH assay, the solution of the enzyme purified in an oxygen-free glove box (0.5 μM finale concentration) was added through a gas-tight syringe to a 0.1 cm light path cuvette prepared in the glove box and containing **HMBPP** (200 μM), NADPH (2.2 mM), flavodoxin (41 μM), flavodoxin reductase (17 μM) in Tris-HCl (50 mM, pH 8) that was previously incubated at 37°C (250 μL final volume). The reaction was monitored photometrically at 340 nm with a Cary 100 UV/visible spectrophotometer (Varian) kept at 37 °C using a thermostat equipped with a Peltier unit. A similar assay was used to determine if **TMBPP** and **AMBPP** were substrates for IspH.

Inhibition assays using [3-^{14}C]HMBPP

[3-^{14}C]HMBPP was synthesized from [2-^{14}C]methyl-D-erythritol 2,4-cyclodiphosphate by incubation with IspG using flavodoxin (FldA), flavodoxin reductase (FpR1) and NADPH as the reductant.[42] Assays were either performed on a Schlenk line under argon or in a glove box under N_2 containing less than 2 ppm O_2. In a typical experiment, a IspH solution (5 μL, 34 nM) was added to samples (95 μL) that contained fixed concentrations of [3-^{14}C]**HMBPP**, NADPH, FldA, FpR1 and varying amounts of **AMBPP** or **TMBPP** in 50 mM Tris-HCl buffer, pH 8 and were pre-incubated for 3 min at 37°C. Incubations were kept at 37 °C for a defined time before addition of 30% trichloroacetic acid (TCA, 5 μL). The quenched assays were neutralized with 1 N NaOH (10 μL), centrifuged and transferred to Eppendorf tubes. Upon verification that the pH was 8, 50 mM Tris-HCl buffer (300 μL, pH 8), containing 5 mM $MgCl_2$ were added followed by *E. coli* alkaline phosphatase (5 μL, 3.1 mg mL^{-1}, 18 units per mg protein, Sigma). The aqueous layers were covered with heptane (800 μL) in order to prevent the loss of volatile products. Samples were incubated at 25 °C overnight. Each sample was extracted with heptane (7 x 600 μL) and the radioactivity of the

combined organic layers was measured using by liquid scintillation spectrometry. A control containing no enzyme was run in parallel.

The radioactivity of assays performed at various inhibitor concentrations, after subtraction of the radioactivity of the control, were plotted as dose-response curves and fit using KaleidaGraph (Synergy software, version 3.5.1 December 2000) according to the equation $y= 1/(1+ (x/IC_{50})^{slope})$ in order to determine the IC_{50} values where y represents the fraction of inhibition and x the inhibitor concentration.

Steady-state kinetic constants were determined from assays at several fixed inhibitor concentrations (15, 30, 50 nM) and varying the substrate concentrations between 0.5 and 4 μM. For the determination of the K_i of **AMBPP** under these conditions, **HMBPP** was used to initiate the pre-incubated reactions. The initial velocities and concentrations were fitted according to the appropriate model of inhibition.[43]

Inhibition assays using dithionite-reduced methylviologen

The activity was measured in a similar manner as first published in reference (25) by using the same IspH and **HMBPP** concentrations as in reference (26) but reducing the dithionite concentration to 0.3 mM. Typically, **HMBPP** (final concentration 34 μM) was added through a gas-tight syringe to a 1 cm light path cuvette prepared in a glove box and containing a mixture of sodium dithionite (0.3 mM), methylviologen (2 mM), IspH (74 nM) and various inhibitor concentrations in 50 mM Tris-HCl buffer pH 8, that was previously incubated for 10 min at 37°C. The reaction was monitored from changes in absorbance at 732 nm ($\varepsilon = 3150\ M^{-1}\ cm^{-1}$) with a Cary 100 UV/visible spectrophotometer (Varian) at 37°C using a thermostat with a Peltier element. Initial velocities at various inhibitors concentrations were plotted as dose-response curves as described above in order to determine the IC_{50} values.

Reversibility of the inhibition

The following steps were carried out in a glove box under nitrogen containing less than 2 ppm of oxygen. IspH (5 μM) was incubated at 37°C for 30 min in the presence of an excess of inhibitor (2 mM) in 50 mM Tris-HCl buffer (pH 8, final volume 250 μL). A portion of the mixture (25 μL) was used to initiate a spectrophotometric assay using NADPH/FpR1/FldA as reducing system in order to verify that the enzyme was completely inhibited. The remaining IspH-inhibitor stock solution was concentrated approximately 5-fold by centrifugation (Microcon® Y-10). Buffer (4 volumes) was then added to the concentrate (1 volume) and the centrifugation-dilution cycle was repeated two more times. The activity of the resulting mixture was assayed as described above. A control sample containing no inhibitor was run under the same conditions.

Slow-binding inhibition

IspH assays in presence of increasing amounts of **AMBPP** (0, 5, 10, 25, 50, 100 μM) were performed using the spectrophotometric assay in presence of NADPH/FpR1/FldA. The reactions were initiated by adding IspH with a gas tight syringe to preincubated mixtures containing NADPH, FpR1, FldA, **HMBPP** and **AMBPP** in 50 mM Tris-HCl buffer. For each recorded absorbance, the absorbance of the control containing no substrate was subtracted. Since addition of IspH and mixing required approximately 30 s, this amount was added to the times for which absorbance was recorded. For each **AMBPP** concentration, the absorbance at t = 0 was estimated from the y-intercept of the straight lines obtained for the first points and y = 0. Progress curves for formation of the product were plotted and fitted with Kaleidagraph according to Eqn (1).

$$P(t)=V_s t+(V_o-V_s)(1-e^{-k_{app}\,x\,t})\times(1/k_{app}) \quad (1)$$

where P(t) is the concentration of product formed (IPP+DMAPP), v_0 and v_s the initial and steady state rates, t the time and k_{app} the apparent first-order rate constant.[29, 28] The dependence of v_0, v_s and k_{app} on the inhibitor concentration [I] permitted to define if the mechanism of inhibition follows mechanism A or B.

Mechanism A

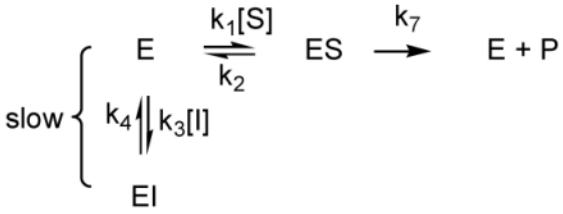

Mechanism B

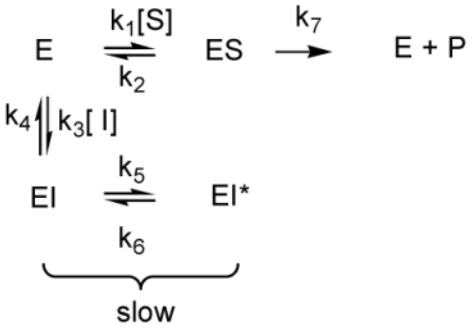

For mechanism A, k_{app} is a linear function of [I] as described in Eqn (2).

$$k_{app}=k_4\{1+[I]/[K_i(1+[S]/K_m)]\} \quad (2)$$

with an inhibition constant $K_i = k_4/k_3$

As the inhibition of IspH by AMBPP followed mechanism A, the fitting of the data to Eqn (2) gave the values for k_4, k_3 and K_i.

For mechanism B, k_{app} is a hyperbolic function of [I] with limiting values of k_6 and k_5+k_6. as described in Eqn (3).

$$k_{app}=k_6\{1+[I]/[K_i^*(1+[S]/K_m)]\}/\{1+[I]/[K_i(1+[S]/K_m)]\} \quad (3)$$

with the initial value for complex formation $K_i = k_4/k_3$ and the final value $K_i^* = K_i[k_6/(k_5+k_6)]$

Supplementary Material

Refer to Web version on PubMed Central for supplementary material.

Acknowledgments

This paper is dedicated to Professor Dr. Wolf-D. Woggon on the occasion of his 70th birthday. We thank Prof. A. Boronat (University of Barcelona, Spain) and his group for providing the *E. coli* strain overexpressing IspH. We are grateful to M. Parisse for technical assistance.

Funding Sources

This work was supported by grants of the 'Agence Nationale de la Recherche' (ANR-05-JCJC-0177-01) to M.S., by the Thai government to K.J, and by National Institutes of Health grant GM 25521 to CDP

References

1. Bloch K. Steroids. 1992; 57:378–383. [PubMed: 1519268]
2. Rohmer M. Nat Prod Rep. 1999; 16:565–574. [PubMed: 10584331]
3. Eisenreich W, Rohdich F, Bacher A. Trends Plant Sci. 2001; 6:78–84. [PubMed: 11173292]
4. Rohmer M, Grosdemange-Billiard C, Seemann M, Tritsch D. Curr Opin Invest Drugs. 2004; 5:154–162.
5. Eisenreich W, Bacher A, Arigoni D, Rohdich F. Cell Mol Life Sci. 2004; 61:1401–1426. [PubMed: 15197467]
6. Missinou MA, Borrmann S, Schindler A, Issifou S, Adegnikz AA, Matsiegui PB, Binder R, Lell B, Wiesner J, Baranek T, Jomaa H, Kremsner PG. Lancet. 2002; 360:1941–1942. [PubMed: 12493263]
7. Borrmann S, Lundgren I, Oyakhirome S, Impouma B, Matsiegui PB, Adegnikz AA, Issifou S, Kun JFJ, Hutchinson D, Wiesner J, Jomaa H, Kremsner PG. Antimicrob Agents Chemother. 2006; 50:2713–2718. [PubMed: 16870763]
8. Borrmann S, Adegnikz AA, Moussavou F, Oyakhirome S, Esser G, Matsiegui PB, Ramharter M, Lundgren I, Kombila M, Issifou S, Hutchinson D, Wiesner J, Jomaa H, Kremsner PG. Antimicrob Agents Chemother. 2005; 50:3749–3754. [PubMed: 16127049]
9. Seemann M, Rohmer M. CR Chimie. 2007; 10:748–755.
10. Gräwert T, Span I, Bacher A, Groll M. Angew Chem Int Ed. 2010; 49:8802–8809.
11. Wolff M, Seemann M, Tse Sum Bui B, Frapart Y, Tritsch D, Garcia-Estrabot A, Rodriguez-Concepción M, Boronat A, Marquet A, Rohmer M. FEBS Lett. 2003; 541:115–120. [PubMed: 12706830]
12. Seemann M, Janthawornpong K, Schweizer J, Böttger LH, Janoschka A, Ahrens-Botzong A, Ngouamegne Tambou E, Rotthaus O, Trautwein AX, Rohmer M, Schünemann V. J Am Chem Soc. 2009; 131:13184–13185. [PubMed: 19708647]
13. Rekittke I, Wiesner J, Röhrich R, Demmer U, Warkentin E, Xu W, Troschke K, Hintz M, No JH, Duin EC, Oldfield E, Jomaa H, Ermler U. J Am Chem Soc. 2008; 130:17206–17207. [PubMed: 19035630]
14. Gräwert T, Rohdich F, Span I, Bacher A, Eisenreich W, Eppinger J, Groll M. Angew Chem Int Ed. 2009; 48:5756–5759.
15. Gräwert T, Span I, Eisenreich W, Rohdich F, Eppinger J, Bacher A, Groll M. Proc Natl Acad Sci USA. 2010; 107:1077–1081. [PubMed: 20080550]
16. Laupitz R, Gräwert T, Rieder C, Zepeck F, Bacher A, Arigoni D, Rohdich F, Eisenreich W. Chem Biodiv. 2004; 1:1367–1376.
17. Wang W, Wang K, Liu YL, No JH, Li J, Nilges MJ, Oldfield E. Proc Natl Acad Sci USA. 2010; 107:4522–4527. [PubMed: 20173096]
18. Dunlap NK, Mergo W, Jones JM, Carrick JD. Tetrahedron Lett. 2002; 43:3923–3925.
19. Outram HS, Raw SA, Taylor JK. Tetrahedron Lett. 2002; 43:6185–6187.

20. Davisson VJ, Woodside AB, Neal TR, Stremler KE, Muehlbacher M, Poulter CD. J Org Chem. 1986; 51:4768–4779.
21. Cramer F, Böhm W. Angew Chem. 1959; 71:775–780.
22. Rohdich F, Zepeck F, Adam P, Hecht S, Kaiser J, Laupitz R, Gräwert T, Amslinger S, Eisenreich W, Bacher A, Arigoni D. Proc Natl Acad Sci USA. 2003; 100:1586–1591. [PubMed: 12571359]
23. Xiao Y, Chu L, Sanakis Y, Liu P. J Am Chem Soc. 2009; 131:9931–9933. [PubMed: 19583210]
24. Gräwert T, Kaiser J, Zepeck F, Laupitz R, Hecht S, Amslinger S, Schramek N, Schleicher E, Weber S, Haslbeck M, Büchner J, Rieder C, Arigoni D, Bacher A, Eisenreich W, Rohdich F. J Am Chem Soc. 2004; 126:12847–12855. [PubMed: 15469281]
25. Altincicek B, Duin EC, Reichenberg A, Hedderich R, Kollas AK, Hintz M, Wagner S, Wiesner J, Beck E, Jomaa H. FEBS Lett. 2002; 532:437–440. [PubMed: 12482608]
26. Wang K, Wang W, No JH, Zhang Y, Zang Y, Oldfield E. J Am Chem Soc. 2010; 132:6719–6727. [PubMed: 20426416]
27. Wang W, Li J, Wang K, Smirnova TI, Oldfield E. J Am Chem Soc. 2011; 133:6525–6528. [PubMed: 21486034]
28. Morrison JF. Trends Biochem Sci. 1982; 7:102–105.
29. Morrison JF, Walsh CT. Adv Enzymol Relat Areas Mol Biol. 1988; 61:201–301. [PubMed: 3281418]
30. Sculley MJ, Morisson JF, Cleland WW. Biochim Biophys Acta. 1996; 1298:78–86. [PubMed: 8948491]
31. Ahrens-Botzong A, Janthawornpong K, Wolny JA, Ngouamegne Tambou E, Rohmer M, Krasutsky S, Poulter CD, Schünemann V, Seemann M. Angew Chem Int Ed. 2011; 50:11976–11979.
32. Citron CA, Brock NL, Rabe P, Dickschat JS. Angew Chem Int Ed. 2012; 51:4053–4057.
33. Span I, Gräwert T, Bacher A, Eisenreich W, Groll M. J Mol Biol. 2012; 416:1–9. [PubMed: 22137895]
34. Xu W, Lees NS, Hall D, Welideniya D, Hoffman BM, Duin EC. Biochemistry. 2012; 51:4835–4849. [PubMed: 22646150]
35. Wang W, Wang K, Span I, Jauch J, Bacher A, Groll M, Oldfield E. J Am Chem Soc. 2012; 134:11225–11234. [PubMed: 22687151]
36. A synthesis of (*E*)-4-amino-3-methylbut-2-enyl 1-diphosphate (AMBPP) was reported[37] while this manuscript was in the final stages of preparation.
37. Das D, Tnimov Z, Nguyen UTT, Thimmaiah G, Lo H, Abankwa D, Wu Y, Goody RS, Waldmann H, Alexandrov K. ChemBioChem. 2012; 13:674–683. [PubMed: 22351497]
38. Bradford MM. Anal Biochem. 1976; 72:248–254. [PubMed: 942051]
39. Fish WW. Methods Enzymol. 1988; 158:357–364. [PubMed: 3374387]
40. Beinert H. Anal Biochem. 1983; 131:373–378. [PubMed: 6614472]
41. Wolff M, Seemann M, Grosdemange-Billiard C, Tritsch D, Campos N, Rodríguez-Concepcíon M, Boronat A, Rohmer M. Tetrahedron Lett. 2002; 43:2555–2559.
42. Seemann M, Tse Sum Bui B, Wolff M, Tritsch D, Campos N, Boronat A, Marquet A, Rohmer M. Angew Chem Int Ed. 2002; 41:4337–4339.
43. Segel, IH. Enzyme Kinetics: Behavior and Analysis of Rapid Equilibrium and Steady-State Enzyme Systems. J. Wiley & Sons, Inc; New York: 1975.

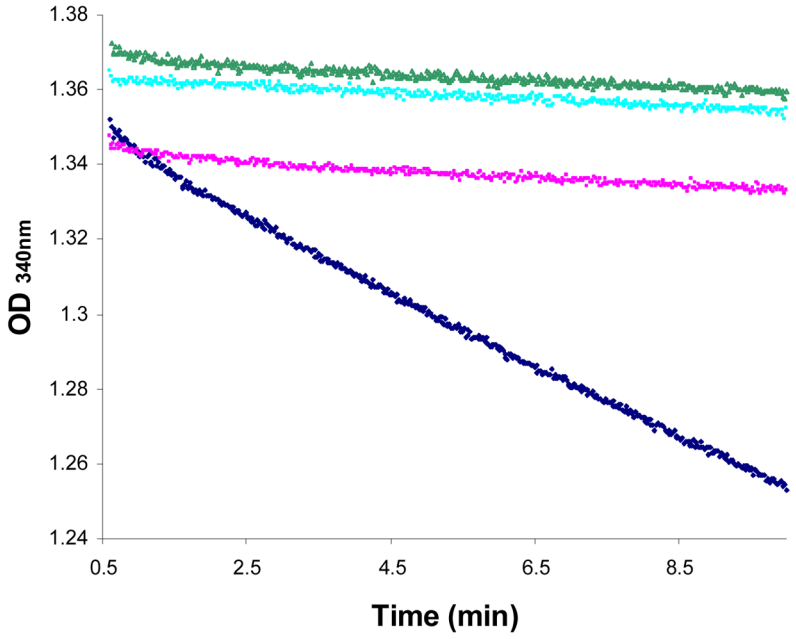

Figure 1.

Decrease of the absorbance of NADPH at 340 nm in the IspH assay using **HMBPP** (dark blue), **AMBPP** (pink), or **TMBPP** (green) as substrates or no substrate (cyan). Conditions: NADPH (2.4 mM), FldA (41 μM), FpR1 (17 μM), and IspH (0.5 μM) in 50 mM Tris HCl buffer, pH 8 (cyan); 200 μM **HMBPP** (dark blue); 200 μM **AMBPP** (pink); 200 μM **TMBPP** (green). Preincubation for 3 min. IspH was added with a gas tight syringe to initiate the reaction. Samples were prepared in a glove box.

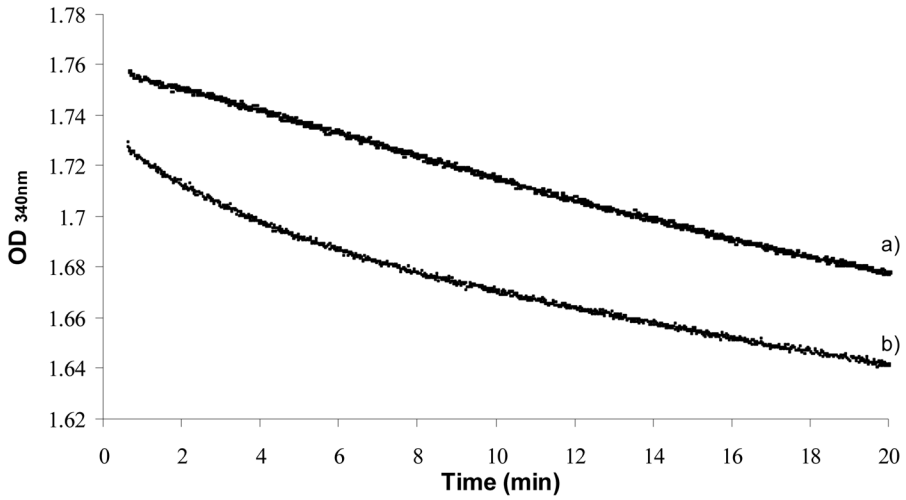

Figure 2.

Inhibition of IspH by **AMBPP** (10 μM) in presence of **HMBPP** (200 μM), NADPH (3 mM), FldA (41 μM), FpR1 (17 μM), IspH (0.5 μM) in 50 mM Tris HCl buffer, pH 8, at 37°C. Preincubation for 10 min with **HMBPP** (a) or IspH (b). Samples were prepared in a glove box and additions were performed with a gas-tight syringe.

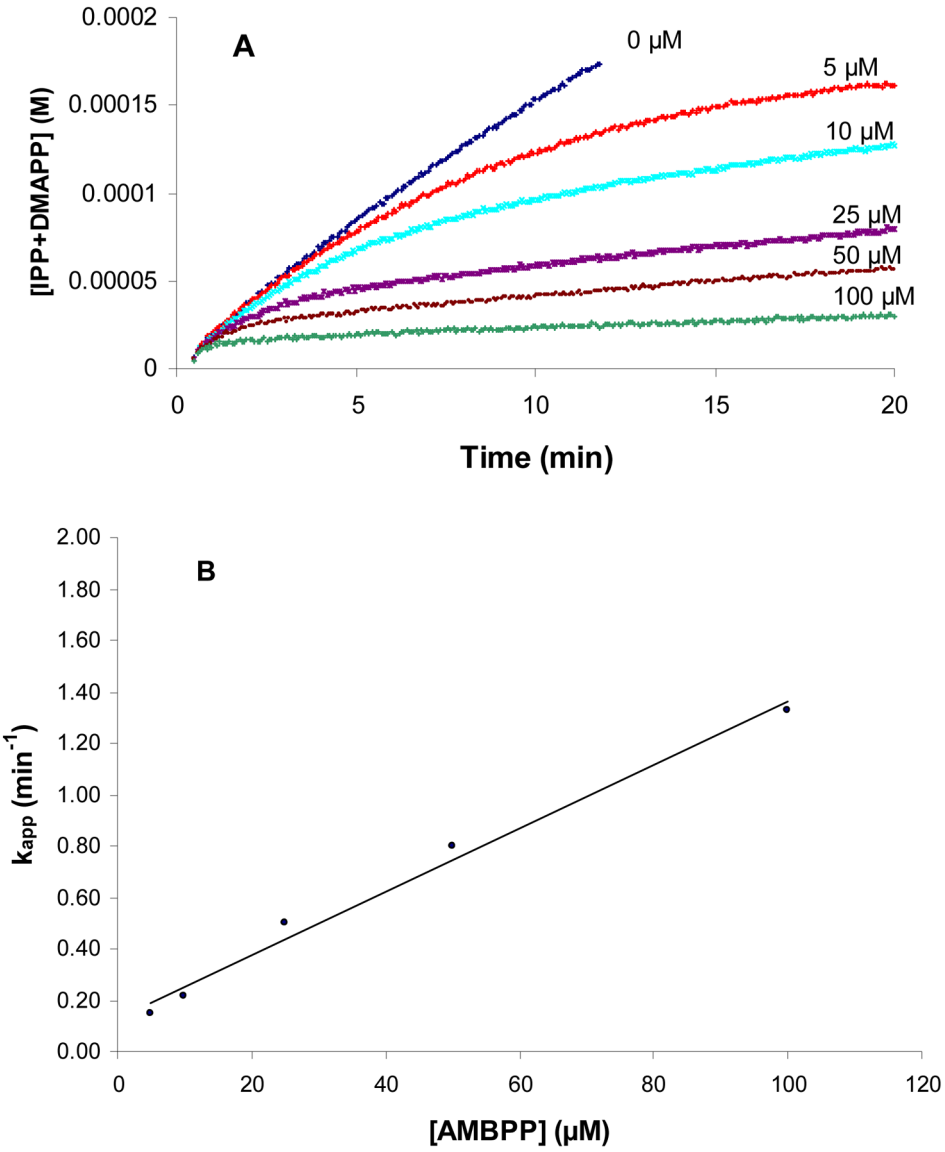

Figure 3.

A) Progress curves for inhibition of IspH by **AMBPP**. The reaction mixture contained NADPH (2 mM), IspH (0.5 μM), **HMBPP** (200 μM), FpR1 (17 μM), FldA (41 μM) in 50 mM Tris HCl buffer, pH 8, and varying concentrations of **AMBPP** from 0–100 μM. After preincubation for 3 min at 37°C, IspH was added with a gas tight syringe to initiate the reaction. Samples were prepared in the glove box. B) A plot of k_{app} vs [**AMBPP**] obtained by fitting the progress curves to Eqn (1).

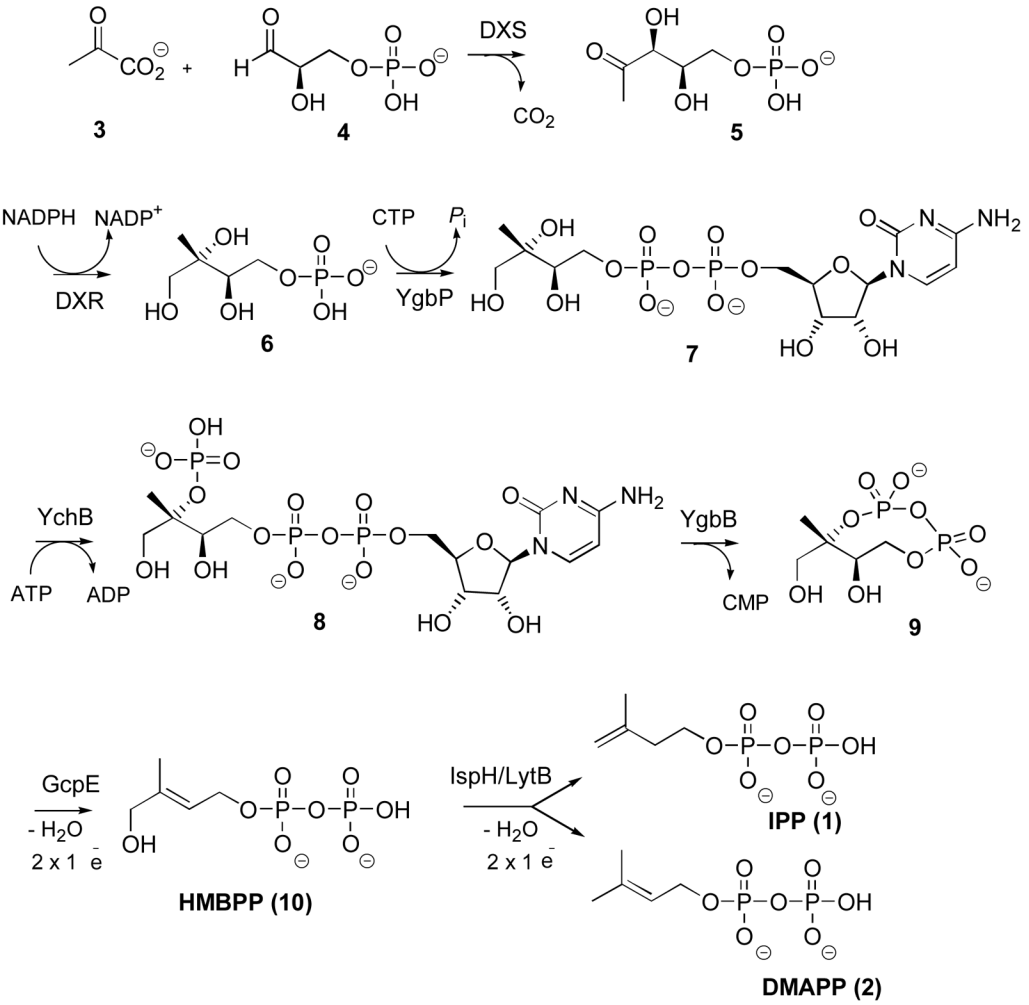

Scheme 1.
Methylerythritol phosphate (MEP) pathway

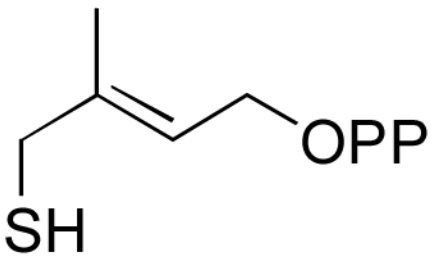

11

TMBPP

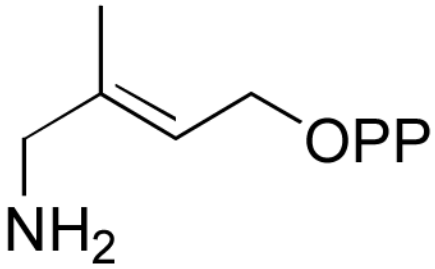

12

AMBPP

Scheme 2.

Structures of the thiol (TMBPP, 11) and amino (AMBPP, 12) analogues of HMBPP

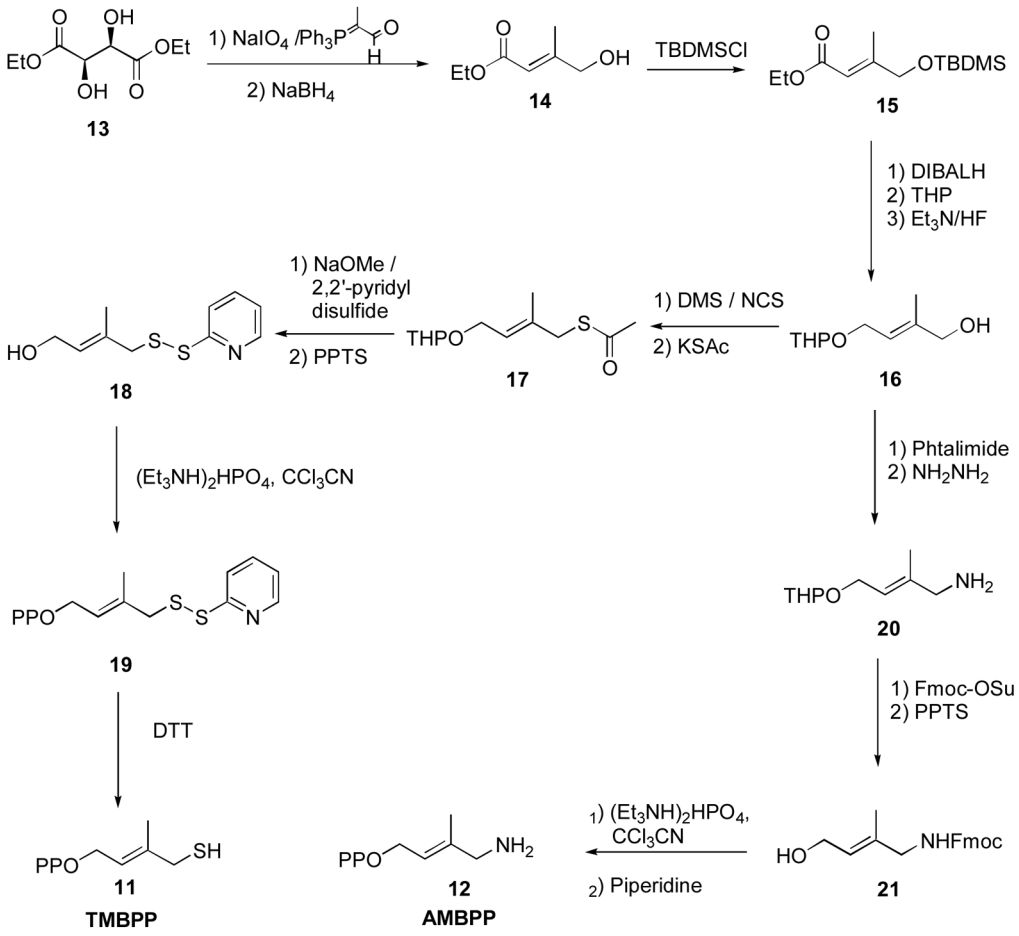

Scheme 3.
Synthesis of TMBPP (11) and AMBPP (12)

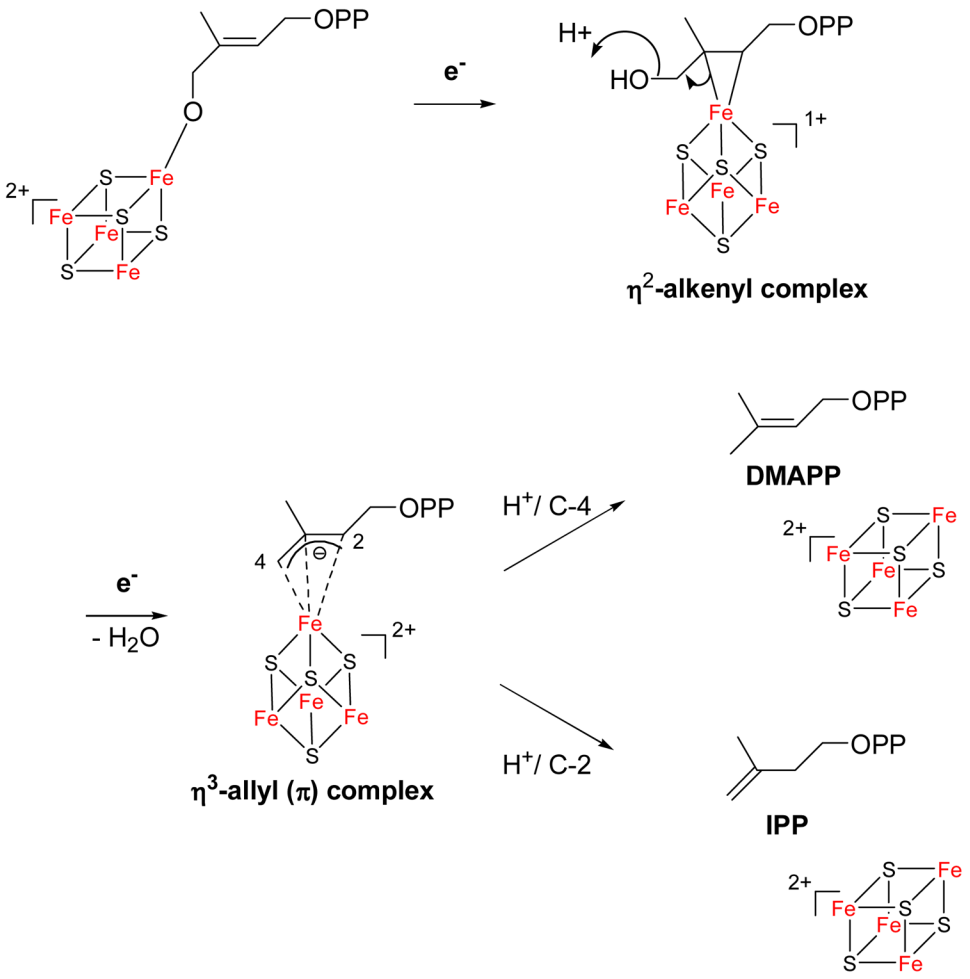

Scheme 4.

Hypothetical biogenetic pathway for the IspH-catalyzed reaction *via* organometallic intermediates

Table 1

IC_{50} values for TMBPP and AMBPP with *E. coli* IspH

Reducing system	TMBPP IC_{50} (nM)	AMBPP IC_{50} (nM)
NADPH/FpR1/FldA[a)]	480 ± 60	390 ± 20
DT-reduced MV[b)]	210 ± 10	150 ± 20

[a)] [3-^{14}C]**HMBPP** (6.2 μCi μmol^{-1}, 9.4 μM), NADPH (6 mM), FldA (15 μM), FpR1 (5 μM), IspH (1.6 nM) and varying amounts of inhibitor in 50 mM Tris HCl buffer, pH 8. IspH was added with a gas tight syringe to initiate the reaction. Incubations were under an argon atmosphere.

[b)] **HMBPP** (34 μM), MV (2 mM), DT (0.3 mM), IspH (74 nM) and varying amounts of inhibitor in 50 mM Tris HCl buffer, pH 8. Preincubation time 10 min at 37 °C. Substrate was added with a gas tight syringe to initiate the reaction. Samples were prepared in a glove box.